JOURNAL OF MATERIALS SCIENCE 17 (1982) 2495–2502

Study of growth rate and failure mode of chemically vapour deposited TiN, TiC_xN_y and TiC on cemented tungsten carbide

J. S. CHO, S. W. NAM, J. S. CHUN
Department of Materials Science, Korea Advanced Institute of Science and Technology, Seoul, Korea

The effects of deposition temperature and mole ratio of CH_4 to $TiCl_4$ on the growth rate of titanium compound coatings were investigated. Activation energies of TiN, TiC_xN_y and TiC deposition reactions of 4.8×10^4, 1.9×10^5 and 2.8×10^5 J mol^{-1}, respectively, were obtained experimentally. The carbon content of TiC_xN_y deposit was increased as the CH_4 flow rate and deposition temperature increased. It was found that TiC_xN_y grain size was finer than TiC and TiN.

The cutting temperatures of TiN-coated and TiC-coated tools were 10% (TiN) and 20% (TiC) lower than that of uncoated tools. Feed force and reaction force of coated tools were 30% and 18% less than those of uncoated tools, respectively. The dominant failure mode of coated tools was due to the microchipping of the cutting edge.

1. Introduction

Recently, there has been wide use of chemical vapour deposition (CVD) techniques to improve the wear resistance of cemented tungsten carbide cutting tools. Titanium carbide, nitride, carbonitride, aluminium oxide and layered combination of these have been used as wear resistant coating materials [1, 2].

There are many publications on the kinetics of coating reactions for CVD TiN [3], TiC_xN_y [4], and TiC [5] on cemented tungsten carbide. However, the relationship of the deposition rate, decarburization zone, and microhardness of TiC to the mole ratio of CH_4 to $TiCl_4$ ($m_{C/Ti}$) has not been clearly established. Therefore, the effects of $m_{C/Ti}$ on the deposition rate, decarburization zone, and microhardness of TiC were investigated. Deposition rate and surface morphology of TiN and TiC_xN_y were examined and compared with TiC.

M. Lee and M. H. Richman [6] suggested that the dominant mode of TiC-coated tool failure might be associated with thermal cracking and microchipping of the cutting edge. We therefore investigated the cutting temperature of coated TiN and TiC on cemented tungsten carbide, and cutting forces of coated tools were measured. These experimental results were compared with an uncoated tool.

2. Experimental procedure

Figure 1 shows the apparatus for CVD of TiN, TiC_xN_y and TiC. A mixture of $TiCl_4$, H_2 and N_2 gases was used for TiN coating, and N_2 was replaced with CH_4 for TiC coating. A mixture of $TiCl_4$, H_2, CH_4 and N_2 was used for TiC_xN_y coating. Deposition was done at ambient pressure, and the reaction temperature was controlled with resistance heating at four temperatures, 1223 K, 1273 K, 1323 K and 1373 K.

Commercial tool inserts of P20 grade, produced by Korea Tungsten Mining Co., were used as the substrates. Standard blank tips, 10 mm × 6 mm × 3 mm, were used in the coating experiments. Throw-away inserts of ISO SNG 432 were used in wear tests.

The coating thickness was determined by two methods; first, the weight increase after coating and second, the observation of the cross-section by optical microscope. The surface morphology

0022–2461/82/092495–08$03.46/0

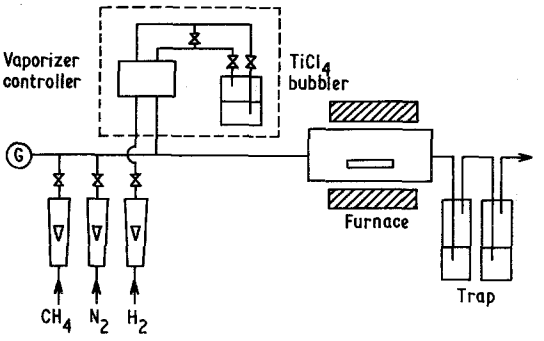

Figure 1 Schematic diagram of CVD apparatus.

of coated layers was observed by scanning electron microscope. The carbon content of TiC_xN_y deposit was determined by an X-ray technique [7]. Microhardness of coated layers was determined by Vickers hardness test under 5.0×10^{-2} kg load.

Outfeed facing operation, as shown in Fig. 2, was used in the evaluation of wear under the following cutting conditions:

workpiece	AISI 1045, 25 mm i.d., 225 mm o.d.
speed	4.2, 10.0 r sec^{-1} (250, 600 r min^{-1})
feed	0.2, 0.3 mm r^{-1}
depth	0.5, 0.9 mm

Wear was measured using a profilometer, and was observed by stereomicroscope. Cutting temperature was measured by tool–workpiece thermocouple, and cutting forces were measured by a three-dimensional dynamometer [8].

3. Results and discussion

3.1. Effect of temperature on the growth rate of TiN, TiC_xN_y and TiC

Figure 3 shows the Arrhenius plots of TiN, TiC_xN_y and TiC deposition rates in the deposition temperature from 1223 K to 1373 K. The activation

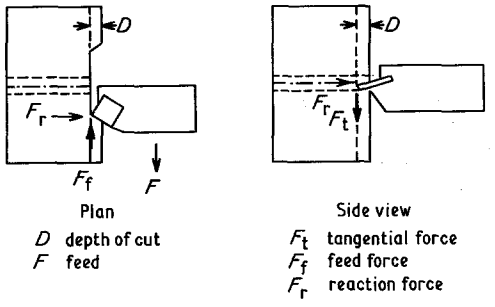

Figure 2 Schematic diagram of outfeed facing operation.

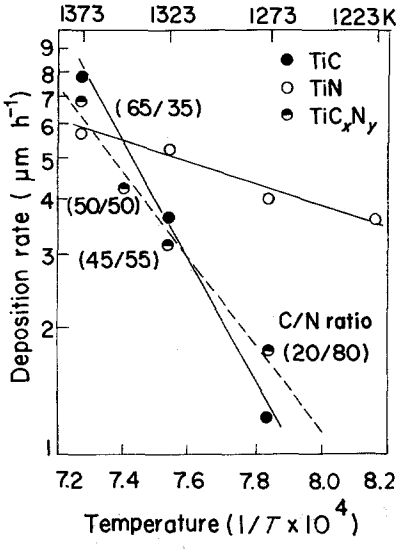

Figure 3 Temperature dependence of TiN, TiC_xN_y and TiC deposition rates.

TiN – H_2 flow rate 5.0 cm^3 sec^{-1}; N_2 flow rate 5.0 cm^3 sec^{-1}; $TiCl_4$ flow rate 0.2 cm^3 sec^{-1}.

TiC – H_2 flow rate 5.0 cm^3 sec^{-1}; CH_4 flow rate 0.5 cm^3 sec^{-1}; $TiCl_4$ flow rate 0.2 cm^3 sec^{-1}.

TiC_xN_y – H_2 flow rate 5.0 cm^3 sec^{-1}; CH_4 flow rate 0.5 cm^3 sec^{-1}; N_2 flow rate 5.0 cm^3 sec^{-1}; $TiCl_4$ flow rate 0.2 cm^3 sec^{-1}.

energy for TiN coating is 4.8×10^4 J mol^{-1} at the flow velocity of 1.9 cm sec^{-1}. This value of 4.8×10^4 J mol^{-1} is in good agreement with T. Sadahiro [3]. He reported that the activation energy of TiN was 5.1×10^4 J mol^{-1} at the flow velocity of 1.3 cm sec^{-1}.

TiC deposition reaction was made with CH_4 flow rate of 0.5 cm^3 sec^{-1}, $TiCl_4$ flow rate of 0.2 cm^3 sec^{-1}. TiC_xN_y deposition reaction was made with the same flow rates of CH_4 and $TiCl_4$, in addition to a flow rate of 5.0 cm^3 sec^{-1} of N_2. The activation energy of TiC deposition reaction is 2.8×10^5 J mol^{-1} and the activation energy of TiC_xN_y deposition reaction is 1.9×10^5 J mol^{-1}. It can be seen in Fig. 3 that the temperature dependence of TiC_xN_y deposition rate was similar to that of TiC. It was found that the carbon content of TiC_xN_y increased with increasing deposition temperature, as determined from the measurement of carbon content by an X-ray technique. These experimental results indicate that the pyrolysis of CH_4 is the main controlling mechanism for both TiC_xN_y and TiC reactions, except in the initial stage in which carbon is provided by diffusion from the substrate until a μm or so of TiC layer has been deposited [15].

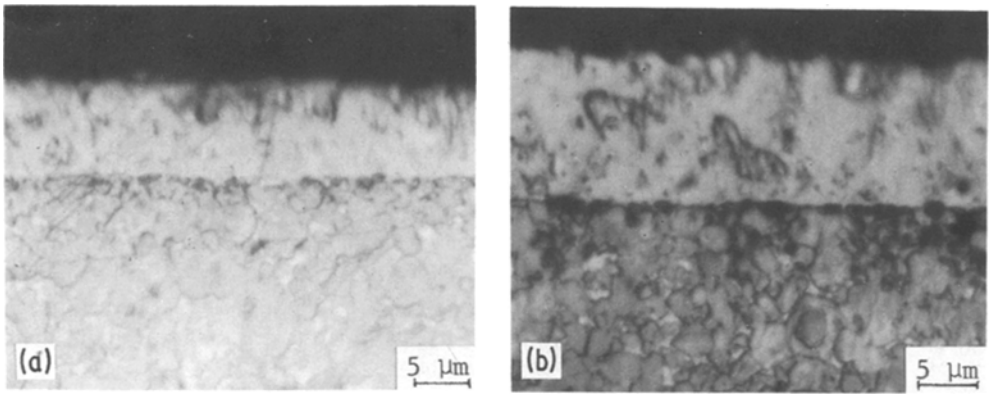

Figure 4 Optical micrographs of cross-sections of TiN coatings. (a) 1223 K; (b) 1273 K.

Figures 4a and b show typical micrographs of TiN deposited at 1223 K and 1273 K, respectively. It can be seen that there is no intermediate layer for TiN coatings deposited at 1223 K, but at 1273 K there is an intermediate layer formed between the TiN coating and the substrate. It is thought that this intermediate layer is probably η-phase, which is produced in TiC coatings, because it appears black when etched with Murakami solution.

Figure 5 shows typical microstructures of TiC, TiN and TiC_xN_y. It reveals that TiC_xN_y has a finer grain microstructure than TiC and TiN.

3.2. Effect of CH_4 on TiC deposition

Figure 6 shows the variation of TiC deposition rate with CH_4 flow rate. At zero mole ratio of CH_4 to $TiCl_4$ ($m_{C/Ti}$) for the substrate reaction, the deposition rate is 0.4 $\mu m\,h^{-1}$. The deposition rate increases to 5.7 $\mu m\,h^{-1}$ at $m_{C/Ti}$ of 3.0, its maximum. Then, the deposition rate decreases for higher $m_{C/Ti}$ values.

Figure 7 shows the optical micrographs of TiC with different values of $m_{C/Ti}$. When the value of $m_{C/Ti}$ is 1.0, shown in Fig. 7a, η-phase exists between the substrate and TiC layer about 8 to 9 μm thickness. However, as $m_{C/Ti}$ increases to the value of 3.0, the thickness of η-phase gradually decreases. A thinner layer of η-phase exists when the value of $m_{C/Ti}$ is greater than 3.0.

Figure 8 shows the microhardness as a function of $m_{C/Ti}$ values. When the value of $m_{C/Ti}$ is less than 3.0, the microhardness of the TiC layer increases to 2800 $kg\,mm^{-2}$ as thickness increases. However, when the value of $m_{C/Ti}$ is more than 3.0, the microhardness decreases. Figure 9 shows the microhardness as a function of thickness deposited at different value of $m_{C/Ti}$. It was found that the microhardness of TiC deposited at $m_{C/Ti}$

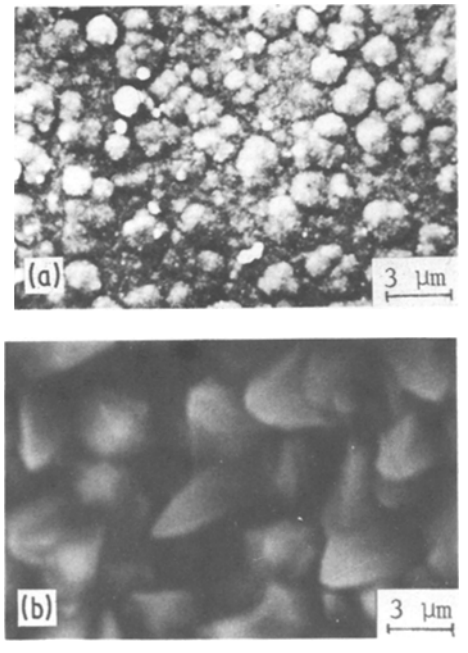

Figure 5 Surface appearance of coating at 1323 K. (a) TiC; (b) TiN; (c) TiC_xN_y.

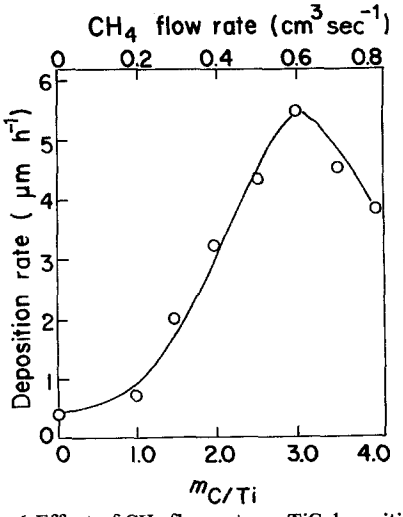

Figure 6 Effect of CH_4 flow rate on TiC deposition rate at 1323 K (deposition temperature 1323 K; time 1 h; H_2 flow rate 5.0 $cm^3 sec^{-1}$; $TiCl_4$ flow rate 0.2 $cm^3 sec^{-1}$; CH_4 flow rate 0 to 0.8 $cm^3 sec^{-1}$).

values greater than 3.0 is less by 300 to 400 kg mm^{-2} than that of TiC deposited at $m_{C/Ti}$ values less than 3.0, at a similar thickness. This is illustrated by two points which have about 4 μm thickness and $m_{C/Ti}$ values of 3.5 and 4.0. The other points in the figure have $m_{C/Ti}$ values less than 3.0.

These results indicate that there is an interrelationship between the variation of growth rate, η-phase and microhardness, and there is a maximum growth rate at proper $m_{C/Ti}$ values. When the value of $m_{C/Ti}$ increases to 3.0, deposition rate and microhardness increase, and the thickness of the η-layer decreases. However, when the value of $m_{C/Ti}$ is more than 3.0, deposition rate and microhardness decrease, and a thinner layer of η-phase occurs.

The zero mole ratio $m_{C/Ti}$ means no CH_4 flow, and $TiCl_4$ gas reacts with carbon from the substrate to form the TiC deposit, but at a very low rate. A similar result has been reported by Lee and Richman [5]. When CH_4 is added, the deposition rate increases as shown in Fig. 6. The deposition rate reaches a maximum at CH_4 flow rate of 0.6 $cm^3 sec^{-1}$ or a mole ratio of 3.0, then decreases with an increase in CH_4 flow rate. The reaction pressure is ambient for all flow rates used.

It is suggested that mole ratio of CH_4 to $TiCl_4$ influences the heterogeneous reaction on the substrate, and homogeneous reaction in the gas phase [9]. The heterogeneous reaction on the substrate is the controlling mechanism at $m_{C/Ti}$ less than 3.0. But homogeneous reaction in the gas phase may be the controlling mechanism at $m_{C/Ti}$ greater than 3.0. Decrease of growth rate at $m_{C/Ti}$ greater than 3.0 is probably due to the supersaturation of

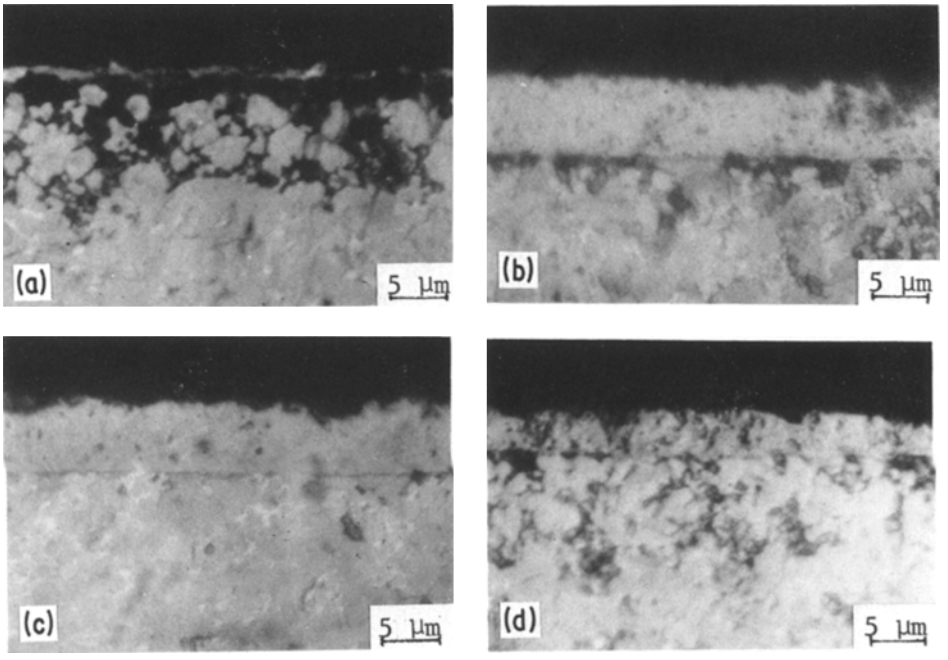

Figure 7 Optical micrographs of cross-sections of TiC coatings. (a) $m_{C/Ti} = 1.0$; (b) $m_{C/Ti} = 2.0$; (c) $m_{C/Ti} = 3.0$; (d) $m_{C/Ti} = 4.0$.

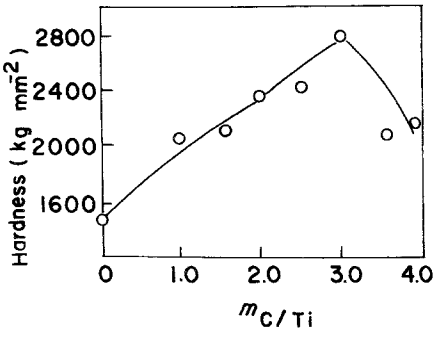

Figure 8 Effect of $m_{C/Ti}$ on the microhardness of TiC coatings (deposition temperature 1323 K; time 1 h; flow rate 5.0 cm^3 sec^{-1}; $TiCl_4$ flow rate 0.2 cm^3 sec^{-1}; CH_4 flow rate 0 to 0.8 cm^3 sec^{-1}).

the CH_4 gas, which results in the production of free carbon that inhibits growth rate. The reason for the decrease of microhardness at above $m_{C/Ti}$ 3.0 as shown in Fig. 9 is due to the powder formation of a coating layer in the homogeneous reaction [9].

3.3. Effect of CH_4 on the growth rate and carbon content of TiC_xN_y

Figure 10 shows the deposition rate and carbon content of TiC_xN_y as a function of CH_4 flow rate at a constant flow of 5.0 cm^3 sec^{-1} of N_2 and at 1323 K. The deposition rate of TiC_xN_y increases with increasing CH_4 flow up to 0.3 cm^3 sec^{-1}, and remains almost constant for further increase of CH_4 flow rate. It is found that the carbon content of TiC_xN_y increases with increasing CH_4 flow rate, and the carbon content of TiC_xN_y can be controlled by CH_4 flow rate.

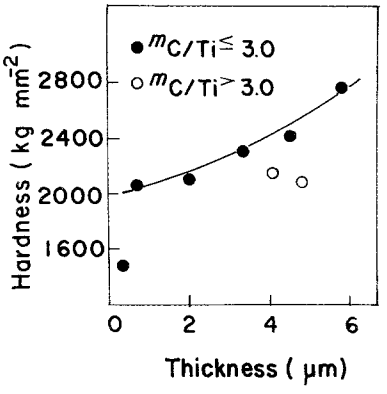

Figure 9 Effect of coating thickness on the microhardness of TiC deposited at different values of $m_{C/Ti}$ (deposition temperature 1323 K; time 1 h; H_2 flow rate 5.0 cm^3 sec^{-1}; $TiCl_4$ flow rate 0.2 cm^3 sec^{-1}; CH_4 flow rate 0 to 0.8 cm^3 sec^{-1}).

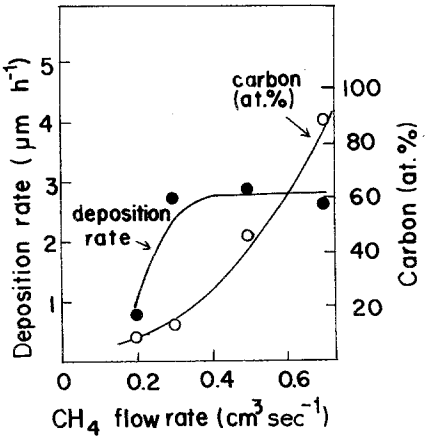

Figure 10 Effect of CH_4 flow rate on the deposition rate and carbon content of TiC_xN_y (deposition temperature 1323 K; time 1 h; flow rate 5.0 cm^3 sec^{-1}; $TiCl_4$ flow rate 0.2 cm^3 sec^{-1}; N_2 flow rate 5.0 cm^3 sec^{-1}; CH_4 flow rate 0 to 0.7 cm^3 sec^{-1}).

3.4. Wear test

Figure 11 shows the cutting temperature against cutting speed plots for uncoated, TiN-coated and TiC-coated tools. It shows that cutting temperature is 8 to 10% lower for TiN-coated tools, and 18 to 22% lower for TiC-coated tools than for an uncoated tool. The TiC-coated tool has the lowest cutting temperature, which is due to a low value of thermal conductivity [10].

Figure 12a shows typical three axial cutting forces against cutting speed plots for the uncoated tool. It shows that the tangential force is the largest among the three forces and almost constant with increasing cutting speed. The feed and reaction forces initially decrease slowly, but increase with cutting speed faster than 2.5 m sec^{-1}. It is believed that the increase of feed and reaction force at faster cutting speed is due to wear increasing rapidly during the cutting operation.

Figure 12b shows typical cutting forces for a TiC-coated tool. It is noted that the cutting forces are similar for TiN-coated, TiC-coated and composite-coated tools. It shows that the feed and reaction forces initially decrease slowly, but are constant with cutting speeds above 2.5 m sec^{-1}. Tangential force is the same as for an uncoated tool. The above results show that feed and reaction forces of coated tools are less by 30% and 18%, respectively, at the cutting speed of 4.7 m sec^{-1}, than those of uncoated tools.

Figure 13 shows typical stereomicrographs of wear shape for TiN-coated, uncoated and TiC-

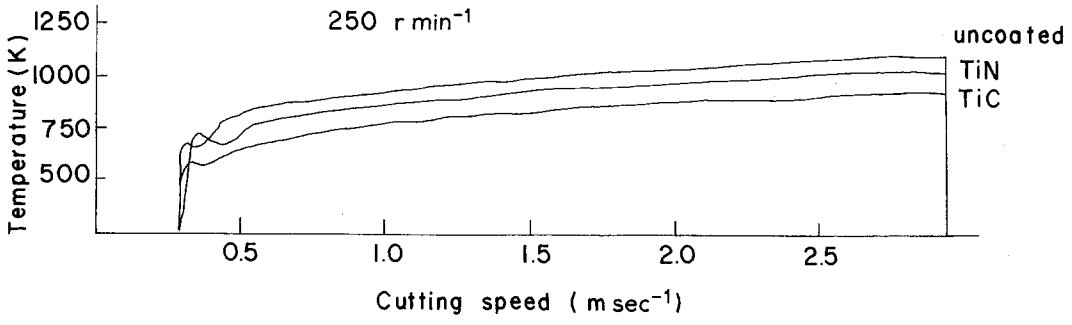

Figure 11 Typical cutting temperatures of uncoated, TiN-coated and TiC-coated tools.

coated tools. It is observed that there is microchipping along the border of the chip flow at the cutting edge for the coated tool.

Figure 14 shows typical optical micrographs of the cross-section of the specimens shown in Fig. 13. It shows that 0.46 mm flank wear land and deep crater wear are produced for an uncoated tool. For the TiC-coated tool, only 0.16 mm of flank wear land and microchipping at the cutting edge are produced. This observation indicates that the dominant mode of coated tool failure is due to the microchipping. It is believed that the formation of microchipping is due to the difference between the thermal expansions of the coating material and the substrate, and the lower value of transverse rupture strength for coated tools [11].

From our experimental results, it can be seen that a composite coating layer of TiC–TiC_xN_y can provide good wear resistance for cutting tools. The difference between the thermal expansion of the substrate and the TiC coating is small, and the cutting temperature is lower due to the low value of thermal conductivity of TiC. In addition, TiC_xN_y coating has a finer grain size than TiC and TiN coatings, which is important in controlling of transverse rupture strength. These factors lead to better wear resistance [2].

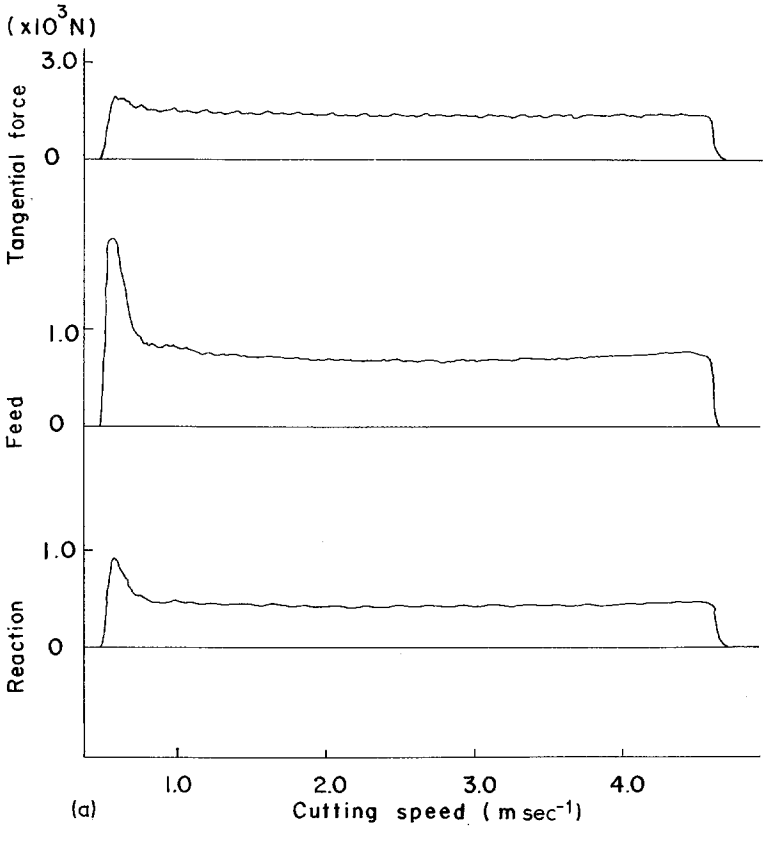

Figure 12 Typical cutting forces of three axes plotted against cutting speed. (a) Uncoated tool; (b) coated tool.

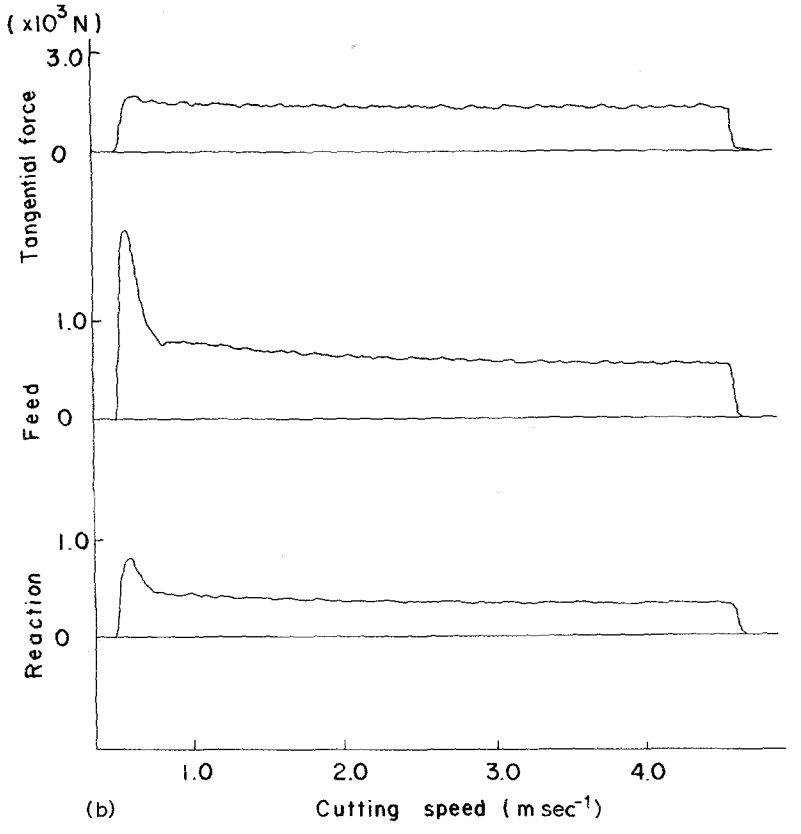

Figure 12 Continued.

4. Conclusions

(1) Activation energies of TiN, TiC_xN_y and TiC deposition reactions were obtained.

(2) When the mole ratio of CH_4 to $TiCl_4$($m_{C/Ti}$) was more than 3.0 for TiC coating, deposition rate and microhardness of the coating layer were decreased.

(3) Carbon content of TiC_xN_y coating layer was increased with CH_4 flow rate and with the deposition temperature.

(4) The dominant failure mode of the coated tool was observed to be associated with the microchipping of the cutting edge.

Acknowledgement

The authors wish to acknowledge KOSEF for supporting this work. The authors also thank Dr James D. Cumming for review and criticism of the manuscript.

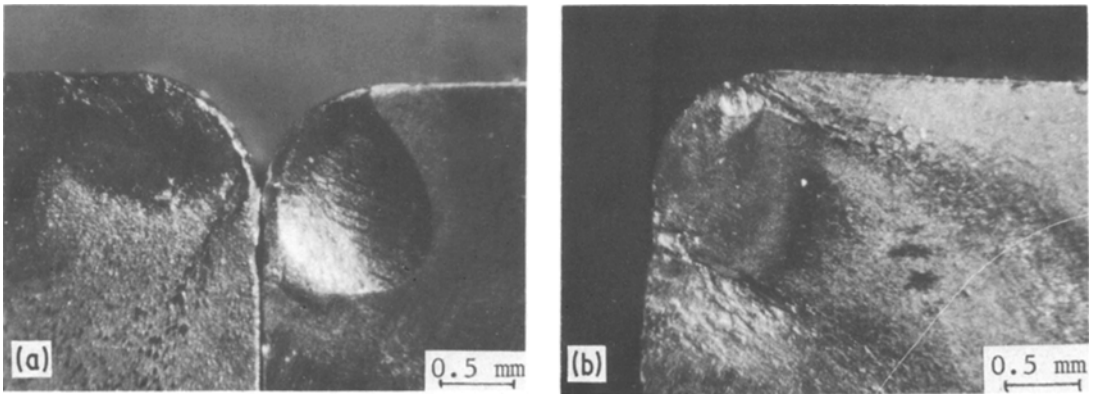

Figure 13 Typical crater wear after wear test. (a) TiN-coated tool (left) and uncoated tool (right); (b) TiC-coated tool.

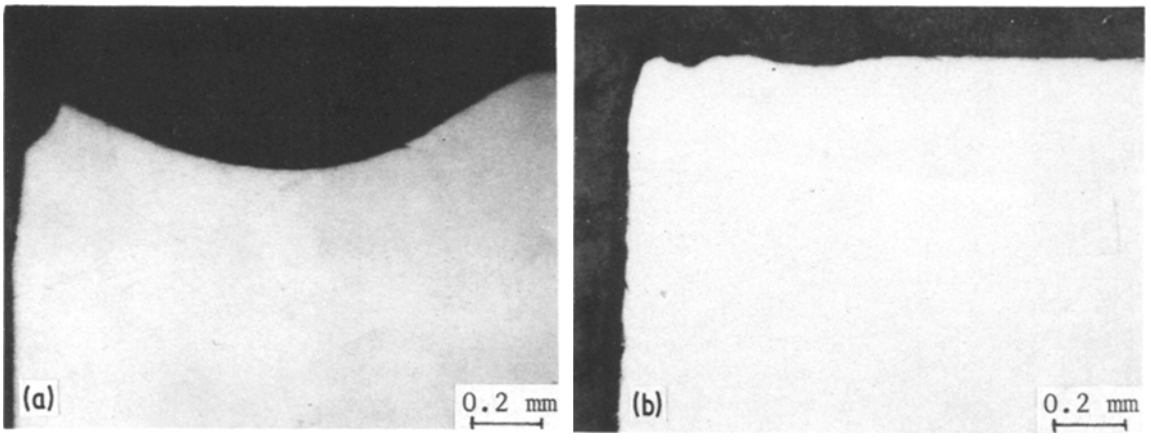

Figure 14 Typical cross-sections of uncoated and coated tools. (a) Uncoated tool; (b) TiC-coated tool.

References

1. P. O. SNELL, *Jernkont, Ann.* **154** (1970) 413.
2. W. S. SCHINTLMEISTER and O. PACHER, *J. Vac. Sci. Technol.* **12** (1975) 743.
3. T. SADAHIRO, T. CHO and S. YAMAYA, *J. Japan Inst. Metals* **41** (1977) 542.
4. G. F. WAKEFIELD and J. A. BLOOM, Proceedings of the 3rd International Conference on Chemical Vapour Deposition, edited by F. A. Glaski (American Nuclear Society, Salt Lake City, Utah, 1972) p. 397.
5. M. LEE and M. H. RICHMAN, *J. Electrochem. Soc.* **120** (1973) 993.
6. *Idem, Met. Technol.* (Dec.) (1974) 538.
7. P. DUWEZ and F. ODELL, *J. Electrochem. Soc.* 97 (1950) 299.
8. G. BOOTHROYD, "Fundamentals of Metal Machining and Machine Tools" (McGraw-Hill, New York, 1975).
9. W. A. BRYANT, *J. Mater. Sci.* **12** (1977) 1285.
10. R. E. TAYLOR and J. MORREALE, *J. Amer. Ceram. Soc.* **47** (1964) 69.
11. W. SCHINTLEMEISTER, O. PACHER, K. PFAFFINGER and T. RAINE, *J. Electrochem. Soc.* **123** (1976) 924.

Received 10 July 1981
and accepted 26 January 1982